DALTON
FULL PAPER

Lanthanide–sulfur gas-phase chemistry: reactions of Ln^+ with S_8 †

Keith Fisher,* Ian Dance and Gary Willett

School of Chemistry, University of New South Wales, Sydney 2052, Australia

All of the lanthanides except promethium have been treated as monocations Ln^+ with S_8(g), in an ion cyclotron resonance mass spectrometer. A rich array of 213 new $[LnS_x]^+$ ions is described. Each lanthanide generates sequences of products $[LnS_x]^+$ in which x generally increases with time. Dominant intermediate ions in these sequences occur with x = 2 (La, Gd), 3 (Eu, Yb), 4 (Nd, Sm, Tb, Dy, Ho, Er, Tm, Lu), 6 (La, Ce, Pr), 9 (Yb), 10 (Nd, Sm, Gd, Tb, Dy, Ho, Er, Tm, Yb, Lu), 11 (Eu), 12 (La, Ce, Pr, Gd), 14 (La) and 18 (Nd). The largest product observed is $[LnS_{21}]^+$ for La and Pr, and the size of the largest ion drops towards the end of the lanthanide series. There is a remarkable similarity between the reactions of Eu^+ (f^7s^1) and Ca^+ (s^1) with S_8: both form $[MS_3]^+$ rapidly, then add S_8 rapidly to form an isomer which can easily dissociate S_8, and also form more slowly a second isomer $[MS_{11}]^+$ which is more stable. Other M^+ with s^1 ground-state configurations do not behave similarly. The smaller $[LnS_x]^+$ probably contain co-ordinated S_2, S_3 and S_4, while some of the larger $[LnS_x]^+$ may contain associated S_8 molecules not bonded directly to Ln. Reaction rates correlate approximately with the occurrence of a ground or low excited state with two unpaired non-f electrons.

The chemistry of the lanthanide elements in condensed phases is dominated by the +3 oxidation state (with significant appearances of oxidation state +2), and the chemical (but not physical) behaviour is characterised by changes of degree rather than of kind. In the gas phase the chemistry of this interlude of elements is distinctly different. The principle effect is that the external stabilisation of the formal +3 and +2 oxidation states is not available, and all of the lanthanides can be prepared as the Ln^+ ions, providing a quite different perspective on lanthanide chemistry. In the gas phase the reactions occur without the influences of extraneous solvents or ligands, and reveal the fundamental reactivities of the lanthanide ions.

In this paper we report and discuss the reactions of Ln^+(g) with elemental sulfur, as S_8 molecules, using Fourier-transform ion cyclotron resonance (FTICR) techniques. This follows our previous investigation of all of the transition elements (except Tc) as monopositive cations with S_8.[1–3]

The gas-phase reactions of Ln^+(g) with organic reactants have been investigated, encompassing 1,3,5-tri-*tert*-butylbenzene,[4] benzene, cyclohexene and cyclohexadiene,[5] alkanes and alkenes,[6–9] and fluorocarbons.[10,11] Carbon–carbon bond formation has been promoted by the reaction of La^+ and Ce^+ with propene in the gas phase,[8] and methane oligomerisation in the gas phase occurs with La^+.[10] Comparative reactivities in these reactions have been interpreted in terms of the electronic configurations of the Ln^+(g) in ground and excited states. However, S_8(g) is a reactant very different from those previously investigated, and we know of no previous investigations with S_8 or indeed any sulfur-containing molecules. Further, while polysulfide chemistry is well developed for the transition metals, pre- and post-transition metals in condensed phases, we are aware of only one investigation[12,13] of lanthanide polychalcogenide chemistry in condensed phases.

Results

In the gas phase at pressures in the range 10^{-6} to 10^{-7} Pa sulfur has been shown to be present solely as S_8 molecules.[1] All of the lanthanides except Pm (which has no natural abundance) were investigated. The ablated ions were collisionally thermalised and relaxed in the ICR cell prior to selection of the Ln^+ ions to be investigated. The disappearance of Ln^+ due to reaction with S_8 showed pseudo-first-order kinetics for all Ln^+, supporting the expectation that a single state of Ln^+ occurs in each case, and this state is assumed to be the ground state. All of the Ln^+ ions formed sequences of products $[LnS_x]^+$, in which x normally increased with time, and smaller intermediates were transformed to larger products. We first describe the rates of initial reaction of bare Ln^+ with S_8, then present the product distributions, and finally describe properties of some intermediates.

Relative reactivities of Ln^+ with S_8

The technique used for generation of S_8(g) did not allow reproducible pressures of S_8 in different experiments, and so in order to measure comparative and absolute reaction rates two strategies were used. In one experiment type the rate of reaction of Ln^+ with S_8 was compared with that of Ar^+ with S_8 under the same conditions. It was assumed that the charge-transfer reaction $Ar^+ + S_8 \longrightarrow Ar + S_8^+$ and the production of smaller S_n^+ ions occurred at collision frequency as the argon has an ionisation energy of 15.5 eV which is considerably greater than that of S_8 (9.04 eV). Therefore the rate of this reaction was taken as the collision rate. The second strategy was to employ internal standards, namely Eu^+ or Lu^+ cogenerated by ablation of their oxide mixed with the precursor of the Ln under investigation, to yield relative rates for all $Ln^+ + S_8$. The electron gun used in experiments with Ar^+ caused the temperature in the cell to be *ca.* 55 °C, compared with *ca.* 25 °C for all other experiments.

Several of the early lanthanide ions were very reactive with background water or oxygen in the cell, forming $[LnO]^+$, $[Sm(OH)]^+$, or $[Eu(OH)]^+$. Where the amount of $[LnO]^+$ was greater than 10%, the rate of the reaction with S_8 was estimated from the formation of products not containing oxygen.

Combination of data from both types of experiment leads to the following semiquantitive results for rates of initial reaction $Ln^+ + S_8$, expressed as a fraction of the collision rate: La, Ce, Tb 0.40; Gd 0.35; Nd, Lu 0.20; Sm 0.15; Dy, Pr 0.12; Er, Eu, Ho, Yb ≈ 0.10; Tm 0.08.

Product distributions

The products of the $Ln^+ + S_8$ reactions are presented in Fig. 1. The $[LnS_x]^+$ products are categorised according to relative abundance as major ions, medium intermediates, and minor

† *Non-SI units employed*: eV ≈ 1.60×10^{-19} J, cal = 4.184 J.

Table 1 Major ions and largest ions $[LnS_x]^+$ formed by reaction of Ln^+ and S_8

Ln^+	Major ions $[LnS_x]^+$ (time period for major abundance)	Highest mass $[LnS_x]^+$ ion	$[MO]^+$ or $[M(OH)]^+$
La	LaS_2 (0–5), LaS_6 (5–20), LaS_{12} (20–50), LaS_{14} (>50)	LaS_{21}	LaO strong
Ce	CeS_6 (0–50), CeS_{12} (>50)	CeS_{20}	CeO strong
Pr	PrS_6 (0–20), PrS_{12} (>20)	PrS_{21}	PrO strong
Nd	NdS_4 (0–10), NdS_{10} (10–50), NdS_{18} (>50)	NdS_{18}	NdO strong
Sm	SmS_4 (0–10), SmS_{10} (>10)	SmS_{18}	Sm(OH) weak
Eu	EuS_3 (0–3), EuS_{11} (>3)	EuS_{19}	Eu(OH) weak
Gd	GdS_2 (0–10), GdS_{10} (10–80), GdS_{12} (>80)	GdS_{18}	GdO medium
Tb	TbS_4 (0–5), TbS_{10} (5–50)	TbS_{16}	TbO medium
Dy	DyS_4 (0–10), DyS_{10} (>10)	DyS_{16}	DyO weak
Ho	HoS_4 (0–10), HoS_{10} (>10)	HoS_{16}	HoO weak
Er	ErS_4 (0–20), ErS_{10} (>20)	ErS_{16}	ErO weak
Tm	TmS_4 (0–5), TmS_{10} (>5)	TmS_{16}	TmO weak
Yb	YbS_2 (0–4), YbS_3 (0–4), YbS_9 (>4), YbS_{10} (>4)	YbS_{15}	YbO weak
Lu	LuS_4 (0–10), LuS_{10} (>10)	LuS_{15}	LuO medium

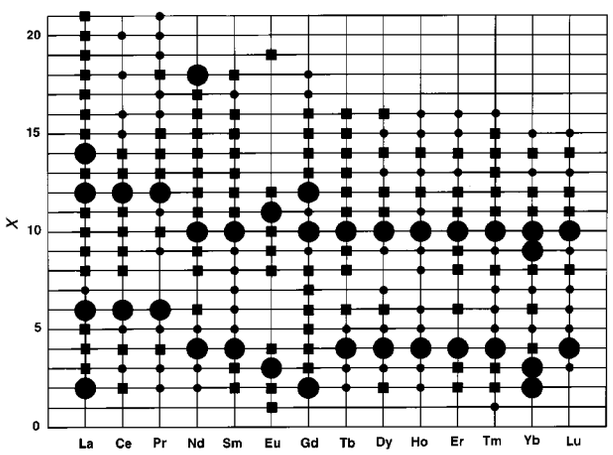

Fig. 1 Map of the observed products $[LnS_x]^+$ formed in reactions of Ln^+(g) (except Pm) with S_8(g). Large circles signify major ions which are dominant at some stage in the reaction, squares represent medium-intensity intermediates (>10%, but not major at any stage), and small circles identify minor ions (<10% intensity)

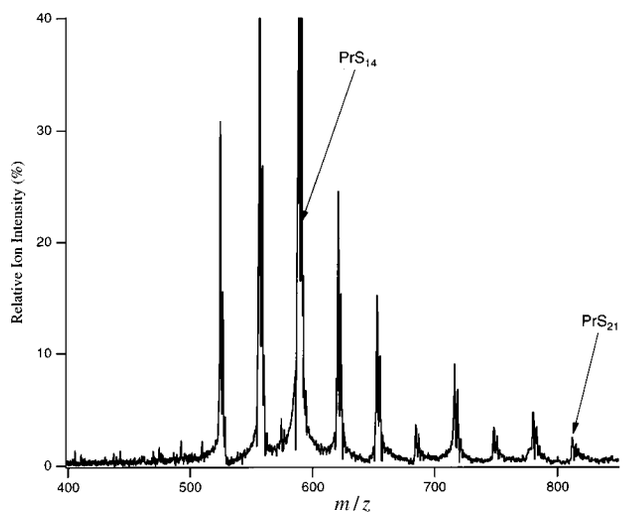

Fig. 2 Products of reaction of Pr^+ with S_8 for 50 s, showing the largest observable ion $[PrS_{21}]^+$

ions. Product ions which are the most abundant at some stage of the reaction sequence are called major ions, the product ions which had a maximum intensity > 10% at some stage but were not major ions are called medium intermediates and minor ions never had relative intensity > 10%. During the course of the reactions the first major ion grew in intensity to a maximum and then decreased as the next major ion became intense. Most reactions were studied for at least 50 s. All Ln^+ formed two or more major ions $[LnS_x]^+$. Table 1 lists the major ions, together with their approximate appearance times, the largest product ion in each case and the products formed by reaction with background oxygen.

The first formed major ions are $[LnS_2]^+$, $[LnS_3]^+$ or $[LnS_4]^+$. We note (see Table 1) that $[LnS_2]^+$ is a major ion for La, Gd and Yb, $[LnS_3]^+$ for Eu and Yb, and that in each case these elements are separated by 7 or 6 in *Z*. The ion $[LnS_4]^+$ occurs more generally as the first major product, for eight of the metals. At longer reaction times $[LnS_{10}]^+$ is a major ion for most of the metals except La, Ce, Pr and Eu. This general occurrence of $[LnS_4]^+$ and $[LnS_{10}]^+$ as major ions is a feature also of the reactions of the transition-metal monocations with S_8.[1] We note also that $[LnS_6]^+$ and $[LnS_{12}]^+$ are major ions for the first lanthanides La, Ce and Pr, and in common with the general $[LnS_4]^+/[LnS_{10}]^+$ pairs of major ions there is also a difference of six in the number of associated S atoms. Europium is distinctive: the major ions are $[EuS_3]^+$ and $[EuS_{11}]^+$, and $[EuS_{19}]^+$ occurs with lower intensity, with an increment of S_8 in each case. At very long reaction times $[EuS_{11}]^+$ adds water to form $[EuS_{11}(H_2O)]^+$. This characteristic is described further below. The S_8 increment is more general: Gd and Yb both show major ions at $[LnS_2]^+$ and $[LnS_{10}]^+$, again with an increment of S_8. Similarly, La which has the only major ion with composition $[LnS_{14}]^+$ also has a major ion $[LaS_6]^+$, again an increment of S_8. Neodymium manifests the largest major ion, $[NdS_{18}]^+$, and also a major ion $[NdS_{10}]^+$ which is separated by S_8.

The products with the largest number of sulfur atoms were $[LaS_{21}]^+$ and $[PrS_{21}]^+$ (see Fig. 2). It is apparent from Fig. 1 that the size of the largest observable ions decreases across the lanthanide series from $[MS_{21}]^+$ observed for La and Pr to $[LuS_{15}]^+$. It can also be noted from Fig. 1 that the compositions $[LnS_5]^+$, $[LnS_7]^+$, and $[LnS_8]^+$ are generally unfavourable in our experiments.

The first four lanthanides, La^+, Ce^+, Pr^+ and Nd^+, react faster with adventitious water than with sulfur. In a control experiment, isolation of La^+ without S_8 yielded $[LaO]^+$ at about the same rate as when S_8 was present. Fig. 3 shows the spectra of Sm^+ and Lu^+ ions reacting for 10 s with S_8 vapor. The Sm^+ and Lu^+ ions were studied under the same conditions, being produced by laser ablation of a mixture of the oxides, followed by isolation of one or the other in the cell. Both metals have $[LnS_4]^+$ as the first major ion which increased to a maximum at about 10 s and then at longer reaction times $[LnS_{10}]^+$ became the major ion. Lutetium had the greater affinity for oxygen as shown by the relative intensity of $[LuO]^+$, while samarium formed the hydroxide ion $[Sm(OH)]^+$ by reaction with the background water. Many of the lanthanide ions form oxo species such as $[LuS_4O]^+$ shown in Fig. 3. These ions were only of significant intensity for the early lanthanides La–Nd, Tb and Lu. The $[LnO]^+$ ions of these metals also react (more slowly than the Ln^+ ions) with S_8.

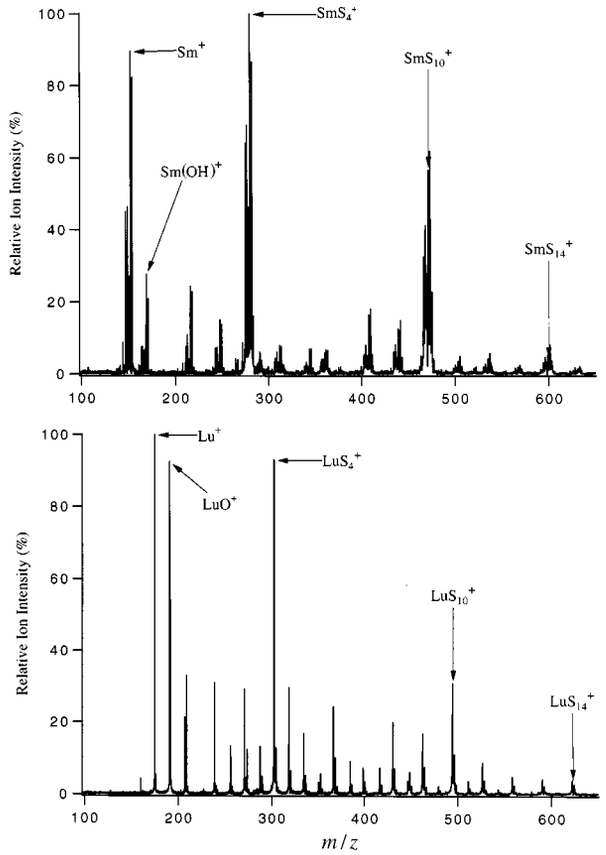

Fig. 3 Products of reaction of Sm^+ or Lu^+ with S_8 for 10 s, under the same experimental conditions. The oxide and hydroxide are due to adventitious water

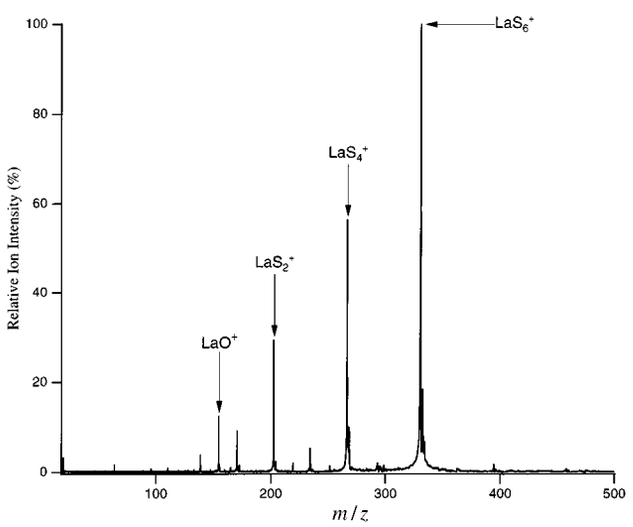

Fig. 4 Dissociation of $[LaS_6]^+$ induced by energised collision with argon

Collision-induced dissociation (CID) experiments

Several major ions $[LnS_x]^+$ were isolated and accelerated in the presence of argon to induce collisional dissociation. Typical of these experiments were the results obtained for $[LaS_6]^+$ shown in Fig. 4. The primary dissociation pathway was the loss of S_2 units. In this context europium was different: CID of $[EuS_3]^+$ caused loss of S_3 to give Eu^+ and the CID of $[YbS_3]^+$ was similar to that of $[EuS_3]^+$. Isolation of $[YbS_4]^+$ and acceleration in the presence of argon gave a 'normal' dissociation pathway to $[YbS_2]^+$ and Yb^+. The CID experiments with $[EuS_{11}]^+$ gave $[EuS_3]^+$ by loss of S_8 (see next section).

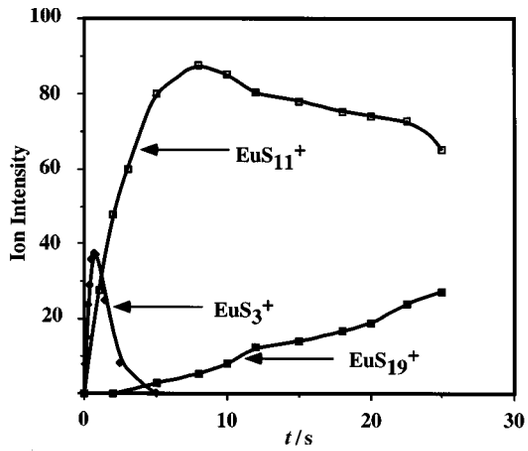

Fig. 5 Temporal evolution of intensities of the major ions in the reaction of Eu^+ with S_8

Reactions of $[LnS_x]^+$

As already mentioned, the product distribution for europium was unique and characterised by increments of S_8. Fig. 5 shows the reaction profile for the major ions $[EuS_3]^+$, $[EuS_{11}]^+$, and $[EuS_{19}]^+$. In the first few seconds $[EuS_3]^+$ grew rapidly and was the major ion, but it was rapidly converted into $[EuS_{11}]^+$ which was then the dominant product for more than 25 s, during which time $[EuS_{19}]^+$ slowly increased in intensity but did not become more abundant than $[EuS_{11}]^+$. Other ions such as $[EuS_9]^+$, $[EuS_{10}]^+$ and $[EuS_{12}]^+$ were present but do not grow to more than 20% of the relative ion intensity.

The $[EuS_3]^+/[EuS_{11}]^+/[EuS_{19}]^+$ sequence was probed further by isolation of the intermediates $[EuS_3]^+$ or $[EuS_{11}]^+$ and observation of their reactions with S_8. The ion $[EuS_3]^+$ reacted to form $[EuS_{11}]^+$, with but small amounts of coproducts $[EuS_9]^+$ and $[EuS_{10}]^+$. Isolated $[EuS_{11}]^+$ on exposure to S_8 dissociated quickly to $[EuS_3]^+$, with about 60% of the $[EuS_{11}]^+$ decomposing in 1 s (see Fig. 6). This was also observed when $[EuS_{11}]^+$ was accelerated and allowed to collide with either argon or sulfur vapor. At longer time periods the intensity of $[EuS_{11}]^+$ increases, and subsequently $[EuS_{19}]^+$ also appears.

Ytterbium is different from the other metals: Yb^+ forms two small products, $[YbS_2]^+$ and $[YbS_3]^+$, at very similar rates, and then these are replaced by another pair of products of similar size, $[YbS_9]^+$ and $[YbS_{10}]^+$, at very similar rates. The temporal evolution of these four products is shown in Fig. 7. Isolated $[YbS_3]^+$ on reaction with S_8 generated mainly $[YbS_{10}]^+$.

Discussion

The questions that arise in this investigation are: (1) what are the patterns of the compositions of the products of reaction of Ln^+ with S_8, and how do they compare with the product distributions for transition and other metals?; (2) what are the structures of the $[LnS_x]^+$ ions?; (3) what are the patterns of reactivity of Ln^+ with S_8, and how can they be rationalised?; (4) what are the implications for the condensed-phase chemistry of the lanthanides? We shall address these questions in turn. Table 2 contains relevant data on the Ln^+ ions.

The lanthanide monocations Ln^+ yield a more extensive and diverse range of $[MS_x]^+$ than do other metals: the matrix of 213 ions in Fig. 1 is impressive. Some of the major compositions, $[MS_4]^+$, $[MS_6]^+$, $[MS_{10}]^+$, $[MS_{12}]^+$, are shared by the transition metals. We note that $[MS_8]^+$ which is a common major ion for the transition metals is a relatively unimportant composition for the lanthanides. Under our experimental conditions the largest size obtainable is greater for the lanthanides ($[LaS_{21}]^+$) than for the transition metals ($[CuS_{16}]^+$). However we believe that the largest size is also determined by the pressure of S_8, and that experiments with higher pressures will yield larger products.

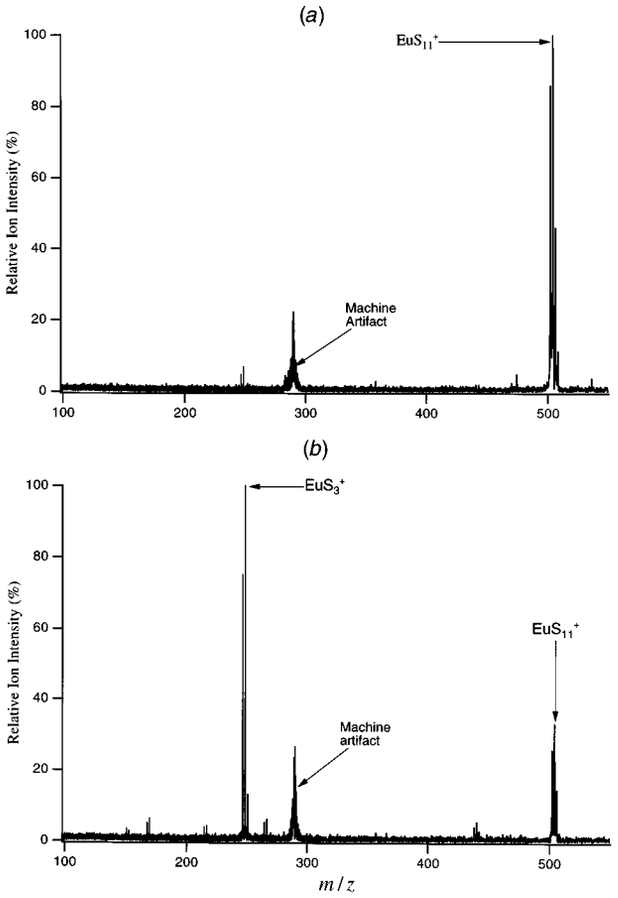

Fig. 6 Mass spectra of $[EuS_{11}]^+$ (*a*) isolated in the cell, (*b*) after reaction with S_8 for 1 s

$$Eu^+ + S_8 \longrightarrow [EuS_3]^+$$

$$[EuS_3]^+ + S_8 \rightleftharpoons [EuS_{11}]^+ \text{ dissociable isomer}$$

$$[EuS_{11}]^+ \text{ dissociable isomer} \longrightarrow [EuS_{11}]^+ \text{ stable isomer}$$

$$[EuS_{11}]^+ \text{ stable isomer} + S_8 \longrightarrow [EuS_{19}]^+$$

Scheme 1

There is an intriguingly close similarity between the reactivities of Eu^+ and Ca^+ with S_8 which is different from those of the transition metals. Both form $[MS_3]^+$ rapidly, then add S_8 rapidly to form $[MS_{11}]^+$ which can easily dissociate S_8, and also form more slowly a second isomer $[MS_{11}]^+$ which is more stable. We believe that the explanation for this anomalous behaviour of Eu^+ is very similar to that previously reported for Ca^+ reacting with S_8.[2] The first formed isomer of $[EuS_{11}]^+$ is postulated to be a weak association of an intact S_8 molecule with $[EuS_3]^+$. The second isomer of $[EuS_{11}]^+$, formed more slowly, involves the breaking of some S–S bonds and formation of some Eu–S bonds.

We have presented density functional calculations of likely structures of $[CaS_3]^+$ and the isomers of $[CaS_{11}]^+$,[2] and postulate similar structures for $[EuS_3]^+$ and $[EuS_{11}]^+$. The larger ion $[MS_{19}]^+$ was not observed with Ca.

We have examined most of the metals of the Periodic Table as monocations reacting with S_8, and Eu, Ca and the other Group 2 metals[14] form a distinctive set. There is well known similarity between the condensed-phase chemistry of Eu^{2+} and Ca^{2+}, and it is evident that the monopositive cations are also closely comparable. To our knowledge, this reactivity with S_8 is the only demonstration of the similarity. The ion Eu^+ has the ground-state configuration $4f^76s^1$, analogous to the $4s^1$ configuration of Ca^+. We note that the other $[LnS_3]^+$ major product occurs for Yb^+ with configuration $4f^{14}6s^1$. We also note that Ca^0 and Eu^0 have very similar radii (1.98 ± 0.01 Å) as do Ca^{2+} and Eu^{2+} (1.1 ± 0.05 Å), and therefore expect that Ca^+ and Eu^+ would have very similar sizes.

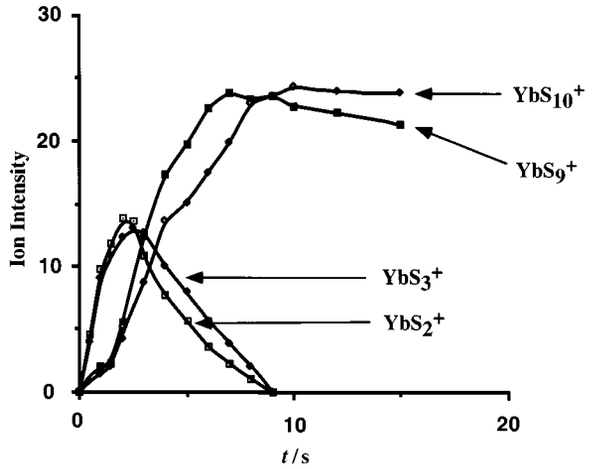

Fig. 7 Temporal evolution of the four major ions formed by reaction of Yb^+ with S_8

Table 2 Data for lanthanide ions (except Pm^+)

Ln^+	Ground-state configuration	Excitation energy/kcal mol^{-1} to $5d^24f^n$	Excitation energy/kcal mol^{-1} to $6s^15d^24f^n$
La	d^2s^0	0.0	4.5
Ce	f^1d^2	0.0	4.7
Pr	f^3s^1	16.1	21.0
Nd	f^4s^1	29.3	34.9
Sm	f^6s^1		54.9
Eu	f^7s^1	106.7	94.2
Gd	$f^7d^1s^1$	12.6	0.0
Tb	f^9s^1	25.4	9.2
Dy	$f^{10}s^1$	58.4	38.7
Ho	$f^{11}s^1$		
Er	$f^{12}s^1$	67.1	29.9
Tm	$f^{13}s^1$	87.9	56.2
Yb	$f^{14}s^1$	128.6	81.7
Lu	$f^{14}s^2$	89.3	37.5

The second question concerns the geometrical structures of the multiple new species we have identified. We usually deploy density functional calculations, with numerical basis sets, to investigate the structures and geometry–energy hypersurfaces of new gas-phase species, but our current methodology is not well able to deal with relativistic effects and we have not yet undertaken calculations on the LnS_x species. We note that the smaller $[LnS_x]^+$ are more abundant for even x, and that collisional dissociation releases S_2, and so for these species it is likely that the Ln atom is surrounded by S_2 groups or S_4 groups, as we have previously described for the transition metals[1] and Freiser and co-workers[15] have shown for $[FeS_n]^+$ (where $n = 2$–10). The collisional dissociation data indicate that $[EuS_3]^+$ and $[YbS_3]^+$ contain intact S_3 ligands, probably as we have described for $[CaS_3]^+$.[2] In the limited number of crystalline lanthanum chalcogenide phases the Ln^{3+} are eight- or nine-co-ordinated by E^{2-} or E_2^{2-} ions,[13] but there are substantial chemical differences between the condensed- and gas-phase compounds and we do not expect close structural similarities.

We consider it likely that some of the larger $[LnS_x]^+$ contain intact S_8 molecules, and cite the facile association and dissociation of S_8 with $[EuS_3]^+$ as evidence. We also raise the possibility that in the very large $[LnS_x]^+$ there are S_8 molecules which are not bonded directly to the Ln atom, but are associated through dispersion forces with the array of S atoms which are directly or indirectly bonded to the Ln atom. This would be a second sphere of S_8 around the inner co-ordination complex. There is precedent for this in the associations of S_8 molecules with C_{60} in the gas[16] and crystalline phases.[17–22] In order to

investigate this hypothesis we plan to undertake experiments at higher pressures of S_8, looking for facile association and dissociation of S_8.

Thirdly, what determines the reactivities and reaction pathways for the different lanthanides with S_8? From prior systematic investigations of the reactivities of Ln^+ with hydrocarbon reactants[4–9] there are two general conclusions: (1) addition reactions are fast, approaching the collisional frequency, and (2) the rates of reactions, requiring disruption of C–H or C–C bonds correlate with the electronic state of the Ln^+ ion, specifically the occurrence of a ground state or low-lying state of Ln^+ possessing two unpaired non-f electrons able to form Ln–C or Ln–H bonds. Thus Schwarz and co-workers[7] correlated inversely the relative reactivities of Ln^+ in activation of organics with the excitation energies to the lowest-lying state with $6s^15d^14f^n$ configuration. Qualitatively the reactivities of Ln^+ with S_8 are similar. The reactions rates are 8 to 40% of collision frequency and there is an approximate inverse correlation of the relative rates with the excitation energies of the lowest $6s^15d^14f^n$ or $5d^24f^n$ configuration (Table 2). Thus the four ions which react most rapidly with S_8 are La^+, Ce^+, Gd^+ and Tb^+, which have states containing two non-f electrons at energies of 0, 0, 0, and 9.2 kcal mol^{-1} respectively.[7] The ions Nd^+, Sm^+, Eu^+, Dy^+, Ho^+, Er^+, Tm^+, Yb^+ and Lu^+ all react more slowly with S_8 and have non-f states all above 29 kcal mol^{-1}; Pr^+ deviates from this correlation, with relatively low reactivity and two low-lying states. Our approximate rate data are generally consistent with the mechanistic hypothesis that two unpaired non-f electrons facilitate the insertion of Ln^+ in a S–S bond as the first stage of reaction with S_8.

Schwarz and co-workers[11] have proposed that the abstraction of an F atom from fluorocarbons by Ln^+ is related to the second ionisation energy of Ln. We see no good correlation of the second ionisation energy with the relative reaction rates with S_8 and also no correlation of the relative reaction rates with the difference between the first and second ionisation energies.

Ytterbium was shown to react differently with fluorobenzene and did so also with S_8. The distinctive observation is the initial formation of two major ions $[YbS_2]^+$ and $[YbS_3]^+$ of similar intensity, and then the formation of two larger ions $[YbS_9]^+$ and $[YbS_{10}]^+$ of similar intensity: this was not observed for other metals, where the major ions are of distinctly higher intensity than other ions formed at similar reaction times. Isolation of $[YbS_3]^+$ and subsequent reaction of this ion with S_8 gave $[YbS_{10}]^+$: this addition of S_7 has not been observed for any other lanthanide or transition-metal ion.

Finally, our results show that in the absence of competing ligands the lanthanide ions could have a rich polysulfide chemistry.

Experimental

Mass spectra were observed using a Spectrospin CM-47 FTICR, and the general methodology was the same as that previously described for the transition metals.[1] Some brief details of the experiments with the lanthanide ions follow. Ions were produced by laser ablation of pressed powdered samples of lanthanum metal oxides or sulfides (La_2S_3, Ce_2S_3) mounted on satellite probe tips and positioned at the end of the ICR cell using a solid insertion probe. The sample was ablated and ionised by a laser pulse focused to an area of ≈0.01 mm^2. Successive laser ablation events occurred at the same spot on the sample.

A Nd-YAG laser (1064 nm) was used in a Q-switched mode (pulse width 8 ns) giving a range of laser powers (150–1770 MW cm^{-2}): most experiments were carried out with a laser power of 770 MW cm^{-2}. Positive ions were trapped in a cylindrical ICR cell (radius 30 × 60 mm) with six titanium single-section plates, in an ultra high vacuum chamber maintained at a base pressure of 10^{-7} Pa by a turbomolecular pump. The trapping potential was +3 V. Sulfur vapor was continually introduced *via* a capillary tube located in the probe tip adjacent to the lanthanide oxide or sulfide to be ablated: the dynamic pressure as recorded on the ion gauge was ≈1×10^{-6} Pa at 25 °C.

Three types of laser ablation experiment were carried out. (1) A lanthanide metal oxide was ablated and the Ln^+ ions trapped in sulfur vapor at ≈1×10^{-6} Pa in the presence of argon making the total pressure 1×10^{-5} Pa. The argon was present to facilitate the collisonal thermalisation and relaxation of the Ln^+ ions prior to investigation. The Ln^+ and the S_8 vapor were allowed to react and the products monitored with reaction time. (2) Since the pressure of S_8 could not be closely controlled, relative rates of reactions of Ln^+ with S_8 were determined by calibration against the rate of reaction of Ar^+ with S_8. The lanthanide metal oxide was ablated in the presence of sulfur and argon at a temperature of ≈55 °C. After monitoring the time decay of Ln^+ due to reaction with S_8, Ar^+ ions were produced by electron impact and rate of reaction of Ar^+ with S_8 under the same conditions was measured. (3) The lanthanide metal oxide or sulfide was mixed with Eu_2O_3 or Lu_2O_3, as secondary standards, and the mixture ablated in sulfur and argon vapors at similar pressures to those in experiment 1. Reactions of Ln^+ with S_8 were measured for each isolated lanthanide ion and the products monitored with time. The reason for this experiment was to calibrate the reaction rate against that for Eu^+ or Lu^+.

Experiments of type 1 and 3 were carried out at ≈25 °C, whereas 2 was only possible using the electron gun, which was operated with a continuous maximum current of 4 A and maintained at a cell temperature of *ca*. 55 °C: the electron gun was shielded when not used to generate Ar^+. In all of these experiments the Ln^+ ions trapped in the ICR cell were first allowed to undergo collisions in the presence of S_8 and argon for at least 1 s before selection of the Ln^+ ion, to permit thermalisation and electronic relaxation of the Ln^+ ions. After this collisional delay the required Ln^+ ion was 'purified' by ejection of all unwanted ions, an event which defined time zero for the subsequently monitored reactions with S_8.

In several cases such as $[LaS_6]^+$, $[PrS_6]^+$ and $[TbS_4]^+$, where the lanthanide has one principal isotope and a tendency to form oxo species, high-resolution and narrow-band spectra were obtained to make sure the products were $[LnS_x]^+$ and not $[LnS_{x-1}O_2]^+$ ions. The isotope patterns of other lanthanide sulfide products (with multiple isotopes) have been examined to ensure the products do not have contributions from H or OH adducts.

In experiments designed to investigate the reactivities of intermediates, the $[LnS_x]^+$ was isolated and allowed to react further with S_8, or accelerated in the presence of argon at 1 x 10^{-5} Pa to study its collision-induced dissociation.

Acknowledgements

This research is funded by the Australian Research Council.

References

1 I. G. Dance, K. J Fisher and G. D. Willett, *Inorg. Chem.*, 1996, **35**, 4177.
2 I. G. Dance, K. J. Fisher and G. D. Willett, *J. Chem. Soc.*, *Chem. Commun.*, 1995, 975.
3 I. G. Dance, K. J. Fisher and G. D. Willett, *Angew. Chem.*, *Int. Ed. Engl.*, 1995, **34**, 201.
4 W. W. Yin, A. G. Marshall, J. Marcalo and A. P. Matos, *J. Am. Chem. Soc.*, 1994, **116**, 8666.
5 J. K. Gibson, *J. Phys. Chem.*, 1996, **100**, 15 688.
6 L. S. Sunderlin and P. B. Armentrout, *J. Am. Chem. Soc.*, 1989, **111**, 3845.
7 H. H. Cornehl, C. Heinemann, D. Schroder and H. Schwarz, *Organometallics*, 1995, **14**, 992.
8 C. Heinemann, D. Schroder and H. Schwarz, *Chem. Ber.*, 1994, **127**, 1807.
9 J. B. Schilling and J. L. Beauchamp, *J. Am. Chem. Soc.*, 1988, **110**, 15.

10 C. Heinemann, N. Goldberg, I. C. Tornieporth-Oetting, T. M. Klapötke and H. Schwarz, *Angew. Chem.*, *Int. Ed. Engl.*, 1995, **34**, 213.
11 H. H. Cornehl, G. Hornung and H. Schwarz, *J. Am. Chem. Soc.*, 1996, **118**, 9960.
12 A. C. Sutorik and M. G. Kanatzidis, *Angew. Chem.*, *Int. Ed. Engl.*, 1992, **31**, 1594.
13 A. C. Sutorik and M. G. Kanatzidis, *Chem. Mater.*, 1997, **9**, 387.
14 K. J. Fisher, I. G. Dance and G. D. Willett, *Rapid Commun. Mass Spetrom.*, 1996, **10**, 106.
15 T. J. McMahon, T. C. Jackson and B. S. Freiser, *J. Am. Chem. Soc.*, 1989, **111**, 421; J. R. Gord and B. S. Freiser, *Anal. Chim. Acta*, 1989, **225**, 11.
16 F. Tast, N. Malinowski, M. Heinebrodt, I. M. L. Billas and T. P. Martin, *J. Chem. Phys.*, 1997, **106**, 9372.
17 G. Roth and P. Adelmann, *J. Phys. I*, 1992, **2**, 1541.
18 N. D. Kushch, I. Majchrzak, W. Ciesielski, A. Graja, K. Wozniak and T. M. Krygowski, *J. Phys. I*, 1987.
19 H. B. Burgi, P. Venugopalan, D. Schwarzenbach, F. Diedrich and C. Thilgen, *Helv. Chim. Acta*, 1993, **76**, 2155.
20 G. Roth, P. Adelmann and R. Knitter, *Mater. Lett.*, 1993, **16**, 357.
21 G. R. P. Adelmann and G. Roth, *Appl. Phys. A*, 1993, **56**, 169.
22 D. Heymann, J. C. Stormer and M. L. Pierson, *Carbon*, 1991, 1053.

Received 1*st September* 1997; *Paper* 7/06349K